

This is the author's peer reviewed, accepted manuscript. However, the online version of record will be different from this version once it has been copyedited and typeset.
PLEASE CITE THIS ARTICLE AS DOI:10.1063/5.0127449

**Spectroscopic Detection of the Stannylidene ($\text{H}_2\text{C}=\text{Sn}$ and $\text{D}_2\text{C}=\text{Sn}$) Molecule
in the Gas Phase**

Tony C. Smith,¹ Mohammed Gharaibeh² and Dennis J. Clouthier^{1a)}

¹*Ideal Vacuum Products, LLC, 5910 Midway Park Blvd. NE, Albuquerque, New Mexico
87109, USA*

²*Department of Chemistry, The University of Jordan, Amman 11942, Jordan*

^aAuthor to whom correspondence should be addressed. Electronic mail:

DJC@Idealvac.com.

This is the author's peer reviewed, accepted manuscript. However, the online version of record will be different from this version once it has been copyedited and typeset.
PLEASE CITE THIS ARTICLE AS DOI:10.1063/5.0127449

Abstract

The H_2CSn and D_2CSn molecules have been detected for the first time by laser-induced fluorescence (LIF) and emission spectroscopic techniques through the $\tilde{B}^1\text{B}_2 - \tilde{X}^1\text{A}_1$ electronic transition in the 425 - 400 nm region. These reactive species were prepared in a pulsed electric discharge jet using $(\text{CH}_3)_4\text{Sn}$ or $(\text{CD}_3)_4\text{Sn}$ diluted in high-pressure argon. Transitions to the electronic excited state of the jet-cooled molecules were probed with LIF, and the ground state and low-lying $\tilde{A}^1\text{A}_2$ state energy levels were measured from single vibronic level emission spectra. We supported the experimental studies by a variety of *ab initio* calculations that predicted the energies, geometries, and vibrational frequencies of the ground and lower excited electronic states. The spectroscopy of stannylidene (H_2CSn) is in many aspects similar to that of silylidene (H_2CSi) and germylidene (H_2CGe).

I. INTRODUCTION

It is well known that acetylene ($\text{HC}\equiv\text{C-H}$) is the global minimum on the H_2C_2 potential energy surface, while vinylidene ($\text{H}_2\text{C}=\text{C:}$) is a higher energy (~ 44.4 kcal/mol) transient intermediate that readily isomerizes to the acetylenic structure.¹ What is perhaps less well recognized is that substitution of a heavier group IV atom into acetylene reverses the energetics, so that silylidene ($\text{H}_2\text{C}=\text{Si}$) and germylidene ($\text{H}_2\text{C}=\text{Ge}$) are the most stable isomers. In 1997, the Clouthier group reported laser-induced fluorescence (LIF) studies of the jet-cooled $\text{H}_2\text{C}=\text{Si}$ and $\text{H}_2\text{C}=\text{Ge}$ molecules,² which turned out to have very interesting spectroscopy and dynamics.

Both silylidene and germylidene have planar ground state geometries of C_{2v} symmetry, with the heteroatom doubly bonded to carbon. Each has a very low-lying \tilde{A}^1A_2 excited state and a much higher energy \tilde{B}^1B_2 excited state. The $S_1 - S_0$ (\tilde{X}^1A_1) electronic transition is orbitally forbidden and is expected to be quite weak, but the $S_2 - S_0$ band system is allowed and enabled the detection of H_2CSi in early flash photolysis absorption experiments.³ We later found that silylidene and germylidene could be readily produced in a pulsed discharge jet from tetramethylsilane (TMS) and tetramethylgermane (TMGe) precursors and they exhibited strong LIF spectra in the blue and near UV regions of the spectrum. Rotational analysis of the 0-0 bands of these species and their deuterated isotopologues showed that the molecules underwent a substantial elongation of the carbon-heteroatom bond and a corresponding diminution of the HCH angle with retention of planar C_{2v} symmetry upon electronic excitation.^{4,5}

The LIF and emission spectra of both silylidene and germylidene show anomalously strong activity in the nontotally symmetric vibrational modes ν_4 (out-of-plane

bend) and ν_6 (CH rocking mode). The ν_6 frequency is unusually small in the ground state and is associated with the isomerization to form the trans-bent HCSiH and HCGeH species, and we attribute the activity in this mode to anharmonicity in the mode 6 potential.^{6,7} In contrast, the out-of-plane bending potential in the excited state appears to be highly anharmonic (the evidence for this is limited but convincing)⁷ and this likely accounts for the activity in ν_4 in the spectra.

Of most interest is the fact that the majority of the rotational levels in the 0-0 bands of both silylidene and germylidene exhibit field-free molecular quantum beats in their fluorescence decays.^{4,5} The patterns are quite beautiful, from simple two-level coupling patterns to those that involve multiple frequency components. Based on density of states arguments, we have concluded that the majority of the beats are due to coupling of excited state levels with high rovibronic levels of the ground state.

In studies of their emission spectra, we were able to observe weak transitions from the \tilde{B} state down to the \tilde{A} states, in the very red end of the spectrum. These were studied at higher resolution by direct LIF spectroscopy and/or stimulated emission pumping (SEP) methods which led to the determination of the molecular geometries and energies of the intermediate \tilde{A}^1A_2 states.^{8,9} In accord with *ab initio* predictions,¹⁰ the C=Si and C=Ge bond lengths elongate (+0.17 Å for both molecules) on promotion of an electron from the π -bonding HOMO to the nonbonding p_y LUMO localized on the heteroatom.

Despite our success in generating H₂CSi and H₂CGe from tetramethylsilane and tetramethylgermane precursors, we originally reported failure² in attempts to observe H₂CSn by LIF spectroscopic probing of the products of a tetramethylstannane discharge.

In the present work, with more sophisticated 2D LIF techniques, we have finally succeeded in observing stannylidene in the gas phase.

II. EXPERIMENT

The reactive stannylidene species were “synthesized” by subjecting tetramethylstannane (TMSn) vapor diluted in an excess of argon to an electric discharge. As described in more detail previously,^{11,12} a General Valve series 9 pulsed molecular beam valve was employed to inject pulses of the gas mixture down a 5 mm diameter flow channel in a Delrin cylinder mounted on the end of the valve. At the appropriate time in the gas pulse, an electric discharge was struck between two stainless steel ring electrodes mounted along the flow channel, fragmenting the TMSn, producing a variety of products. These products were cooled by the expansion of the high-pressure gas pulse into vacuum at the exit of the flow channel. A 1.0 cm long, 0.5 cm internal diameter reheat tube¹³ was attached to the end of the flow channel to suppress the excited argon glow and increase the production of the species of interest.

Since our previous attempt to observe H_2CSn failed, we decided that it would be crucial to probe the discharge products with the highest possible sensitivity over a broad range of wavelengths, rather than limiting our investigations to LIF probing of specific regions with a dye laser. For this purpose, we employed a broadly tunable and highly sensitive 2D LIF spectrometer developed in our laboratory based on an optical parametric oscillator (OPO-A, GWU-Lasertechnik, 400-710 nm, linewidth 2 - 5 cm^{-1} , energy 10-50 mJ/pulse). The horizontally oriented TMSn discharge expansion was crossed at right angles with the horizontally propagating laser beam and any resulting fluorescence was

imaging vertically upwards through appropriate long-pass filters onto the photocathode of a red sensitive photomultiplier (RCA C31034A PMT). Simultaneously, emission in the downward direction was collected with a lens and imaged onto the slit of a scanning monochromator (Spex 500 M) equipped with a 300 line/mm grating blazed at 500 nm. The dispersed emission spectrum was detected with an intensified, gated CCD detector (Andor iStar 320T, wavelength range of photocathode 260-850 nm). The OPO wavenumbers were calibrated with simultaneously recorded neon optogalvanic lines and the emission spectra with argon lines from a Li/Ar hollow cathode lamp.

In operation, the 2D LIF spectrometer recorded two dimensions of data: the total LIF signal, and the dispersed emission spectrum at each laser step. Ten long pass filters mounted in a motorized filter wheel (ThorLabs CFW 3-10) and computer selected as the laser scanned were used to suppress the scattered laser light contribution to the LIF signal. In order to record weak signals, the LIF signal was averaged for an extended period (typically 100 – 500 laser shots) and at the same time the emission spectrum was accumulated on the CCD, gated 6-8 ns after the laser pulse out to $\sim 8 \mu\text{s}$. Once the averaging was complete, the total LIF signal was recorded and the corresponding emission spectrum was read from the CCD. The process was repeated by moving the laser to the next position (typically 2-3 cm^{-1} to the blue of the previous point), the monochromator center wavenumber was incremented by the same amount to keep a constant offset (in cm^{-1} units) between the laser and the emission spectrum, and the averaging continued. The laser-induced fluorescence, emission and calibration spectra were digitized and recorded simultaneously on a computerized data acquisition system of our own design. The 2D spectra were displayed as a plot of laser wavenumber vs total fluorescence intensity (the

LIF signal) and vs dispersed fluorescence color-coded intensity as a function of displacement from the laser. The 2D LIF experiments were time-consuming and were usually run overnight, generating massive data sets which could be post-processed to enhance or suppress individual signals.

Subsequent to the 2D LIF studies, higher resolution (0.1 cm^{-1}) survey LIF spectra were recorded using a neodymium: yttrium aluminum garnet (Nd:YAG) pumped dye laser (Lumonics HD-500) excitation source in the same apparatus as described previously. The spectra were calibrated with optogalvanic lines from various argon- and neon-filled hollow cathode lamps to an estimated absolute accuracy of 0.1 cm^{-1} .

For emission spectroscopy, previously measured LIF band maxima were excited by the dye laser and the resulting fluorescence was imaged with $f/4$ optics onto the entrance slit of a 0.5 m scanning monochromator (Spex 500M). The emission spectra were calibrated to an estimated accuracy of $\pm 1 \text{ cm}^{-1}$ using emission lines from an argon-filled hollow cathode lamp. A 1200 line/mm grating blazed at 500 nm was employed in this work, which gave a bandpass of 29.9 nm with an 18 mm effective active area on the CCD.

Tetramethylstannane [TMSn or $(\text{CH}_3)_4\text{Sn}$, Sigma-Aldrich, 97%], was used as received. Tetramethylstannane- d_{12} [TMSn- d_{12} or $(\text{CD}_3)_4\text{Sn}$] was synthesized by the spontaneous reaction of tin tetrachloride (Sigma-Aldrich) and dimethylcadmium- d_6 . Appropriate amounts of the two reactants were condensed into an evacuated tube with liquid nitrogen, the tube was sealed with a Teflon stopcock and the reaction mixture allowed to warm to room temperature over a period of ~ 1 hour. The volatile components (primarily the desired product) were pumped off and purified by trap-to-trap distillation under vacuum. Dimethylcadmium- d_6 was made by the reaction of cadmium chloride

(CdCl₂) with magnesium Grignard CD₃MgI.¹⁴ The purity of all synthesized materials was checked by gas-phase infrared spectroscopy.

In practice, the TMSn or TMSn-d₁₂, stored in a Pyrex U-tube, was degassed to remove any traces of dissolved oxygen and then diluted with 40-50 psi of argon. The argon entrained TMSn vapor (room temperature vapor pressure ~ 90 Torr) and the gas mixture flowed through stainless steel tubing to the pulsed valve.

III. *AB INITIO* CALCULATIONS

As a preliminary to our experimental efforts, we conducted a theoretical study of the ground and excited states of H₂CSn, D₂CSn and their geometric isomers. The aim was not to do an extensive, comprehensive investigation, as we did, for example, on AlCH₂,¹⁵ but rather to provide enough information about the energies of the electronic states, their molecular structures and vibrational frequencies, and the expected spectra to support the experimental inquiries.

Tin has ten naturally occurring isotopes of which seven have abundances greater than 4%, with the most prominent being ¹²⁰Sn = 32.6% and ¹¹⁸Sn = 24.2%. All of our calculations were done on molecules incorporating the ¹²⁰Sn isotope. First, we performed a series of density functional theory (DFT) calculations using the GAUSSIAN 09 program suite¹⁶ with the Becke three-parameter hybrid density functional,¹⁷ the Lee, Yang, and Parr correlation functional¹⁸ (B3LYP), and Dunning's correlation consistent basis sets augmented by diffuse functions (aug-cc-pVTZ).¹⁹ For the tin atom, an effective core potential (ECP) approach was adopted, using the aug-cc-pVTZ-pp basis set.²⁰ The geometric parameters of the three states were optimized, and the vibrational frequencies

were calculated. In addition, higher-level coupled-cluster singles and doubles with triples added perturbatively [CCSD(T)] calculations of the same properties were also performed.

As there were few previous theoretical calculations of the H_2CSn species, we first investigated the stability of potential isomers, as summarized in Table I. In what follows,

TABLE I. The Sn-C bond lengths and relative energies (CCSD(T), B3LYP in parentheses) of the lowest singlet states of the various $\text{H}_2\text{C}^{120}\text{Sn}$ geometric isomers.

Isomer	r(Sn-C) Å	Relative Energy (kcal/mol)
H_2CSn planar singlet	2.009 (2.002)	0.0 (0.0)
HSnCH trans-bent singlet ^a	1.932 (1.933)	52.4 (61.4)
CSnH_2 planar singlet ^a	2.063 (2.046)	120.9 (116.4)

^a A nonplanar triplet state of slightly lower energy was found at the B3LYP level but could not be confirmed with CCSD(T).

we denote the results of the two levels of theory investigated as CCSD(T)/B3LYP, both with the same basis sets. In all cases, the planar singlet H₂CSn structure of C_{2v} symmetry was found to be the global minimum with six real vibrational frequencies and a C=Sn bond length of 2.009/2.002 Å. The corresponding C_{2v} triplet state, formed by the promotion of an electron from the C-Sn π orbital to the empty 5p orbital on the tin atom, is 25.4/21.4 kcal/mol higher in energy with an elongated C-Sn bond (0.149/0.176 Å longer), precisely as found previously.²¹

In 2011, Wu and Su²² reported DFT calculations indicating that singlet HCSnH and CSnH₂ were also higher energy stationary points on the potential energy surface. We concur, with the singlet HC=SnH stanylacetylinic isomer at 52.4/61.4 kcal/mol and singlet CSnH₂ 120.9/116.4 kcal/mol above the global minimum. No stable linear acetylenic structure (HSnCH) was found.

The spectroscopic parameters calculated for the ground and excited states of H₂C=Sn are collected in Table II. Our previous experience with calculations on tin dihydride²³ showed that CCSD(T) energies were seriously in error in locating the excited state. Since the whereabouts of the stannylidene excited states was crucial for the present work, we also used the symmetry adapted cluster-configuration interaction (SAC-CI) method implemented in GAUSSIAN 09 to hopefully obtain better predictions. The geometries of the ground and first two excited singlet states were optimized and the difference of the energies was used to predict T_e . These were corrected to T_0 values using the DFT vibrational frequencies, with the results given in Table II.

The ground state molecular orbital configuration of stannylidene is

$$\dots(b_2)^2(a_1)^2(b_1)^2(b_2)^0$$

TABLE II. *Ab Initio* spectroscopic parameters [CCSD(T) with B3LYP in parentheses, SAC-CI in boldface] for the ground and excited states of planar C_{2v} stannylidene. Vibrational frequencies and T_0 (in cm^{-1}) are listed as $\text{H}_2\text{C}^{120}\text{Sn}/\text{D}_2\text{C}^{120}\text{Sn}$.

Parameter	\tilde{X}^1A_1	\tilde{a}^3A_2	\tilde{A}^1A_2	\tilde{B}^1B_2
$r(\text{CSn}) \text{ \AA}$	2.009 (2.002) 2.000	2.159 (2.178) 2.158	2.163 (2.179) 2.150	2.043 (2.085) 2.084
$r(\text{CH}) \text{ \AA}$	1.090 (1.087) 1.090	1.089 (1.088) 1.089	1.090 (1.088) 1.088	1.079 (1.076) 1.076
$\theta(\text{HCH})^\circ$	113.2 (113.3) 114.0	112.4 (112.4) 112.4	112.5 (112.5) 111.9	129.9 (134.8) 134.4
$\omega_1 (a_1)$ symm. CH stretch	3079/2233 (3082/2235)	3075/2227 (3063/2218)	3072/2225 (3063/2217)	3161/2266 (3140/2247)
$\omega_2 (a_1)$ symm. CH bend	1346/1020 (1340/1017)	1390/1038 (1376/1027)	1388/1035 (1374/1026)	1166/856 (1157/858)
$\omega_3 (a_1)$ Sn-C stretch	665/610 (678/621)	547/510 (525/489)	542/505 (522/487)	580/555 (511/485)
$\omega_4 (b_1)$ out-of-plane bend	641/501 (648/507)	574/448 (575/448)	596/465 (584/455)	629/516 (574/444)
$\omega_5 (b_2)$ antisymm. CH stretch	3166/2349 (3166/2349)	3166/2352 (3153/2343)	3163/2349 (3152/2342)	3332/2497 (3356/2518)
$\omega_6 (b_2)$ antisymm. CH bend	392/295 (426/320)	583/436 (584/437)	589/441 (588/440)	595/445 (649/479)
T_0	---	8922/8901 (7461/7449) 8962/8950^b	9267/9243 (7634/7621) 10016/10004^b	20992/20949 (19774/19741) 23928/23895^b
Dipole Moment (Debye) ^a	(+1.18)	(-0.52)	(-0.44)	(+0.68)

^aA positive value has the positive end of the dipole pointing along the C-Sn bond towards

This is the author's peer reviewed, accepted manuscript. However, the online version of record will be different from this version once it has been copyedited and typeset.
PLEASE CITE THIS ARTICLE AS DOI:10.1063/5.0127449

This is the author's peer reviewed, accepted manuscript. However, the online version of record will be different from this version once it has been copyedited and typeset.
PLEASE CITE THIS ARTICLE AS DOI:10.1063/5.0127449

the Sn atom. Negative values are the reverse.

^bCalculated using SAC-CI electronic energies and B3LYP vibrational frequencies.

where the b_2 orbital is predominantly an in-plane p orbital on carbon, the a_1 orbital is a sigma-type orbital with a buildup of electron density between C and Sn and between the two hydrogens, the b_1 orbital is a carbon-tin π bonding orbital, and the unoccupied b_2 orbital is essentially an in-plane p_y orbital on the tin atom. The shapes and orientation of the molecular orbitals are illustrated in Fig. 1.

Promotion of an electron from the highest occupied molecular orbital (HOMO) of b_1 symmetry to the b_2 lowest unoccupied molecular orbital (LUMO), a $\pi \rightarrow n$ transition, yields low-lying \tilde{a}^3A_2 and \tilde{A}^1A_2 excited states. The next lowest energy singlet state involves promotion of an electron from the second highest occupied molecular orbital (SHOMO a_1) to the LUMO (b_2), yielding a \tilde{B}^1B_2 excited state. As summarized in Fig. 1, the $\tilde{A} - \tilde{X}$ transition is electric dipole orbitally forbidden and is expected to be very weak, although it may gain intensity by vibronic coupling with the \tilde{B} state. The $\tilde{B} - \tilde{X}$ transition is allowed with the transition moment along the b inertial axis, giving B -type perpendicular bands. The emission transitions from the \tilde{B} state down to both the \tilde{X} and \tilde{A} states are allowed and should be observable.

Our best theoretical estimate (SAC-CI) of the location of the $\tilde{B}-\tilde{X}$ 0-0 band of $H_2C^{120}Sn$ is $23\,928\text{ cm}^{-1}$, in close agreement with the *ab initio* value of $23\,472\text{ cm}^{-1}$ given by Harper *et al.*² in their original communication on the discovery of the spectra of jet-cooled H_2CSi and H_2CGe . The forbidden $\tilde{A}-\tilde{X}$ transition is predicted at $10\,016\text{ cm}^{-1}$ (998 nm), well outside the range of conventional dye lasers and photomultiplier detectors. However, the $\tilde{B} - \tilde{A}$ 0-0 band emission is calculated at $23\,928 - 10\,016$ (SAC-CI, Table I)

This is the author's peer reviewed, accepted manuscript. However, the online version of record will be different from this version once it has been copyedited and typeset.
PLEASE CITE THIS ARTICLE AS DOI:10.1063/5.0127449

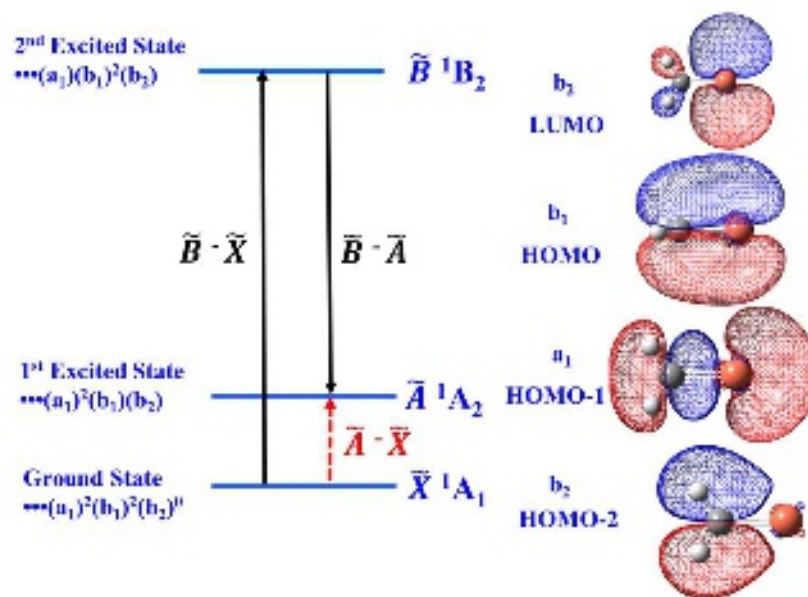


FIG. 1. Schematic diagram showing the ground and low-lying electronic singlet states of H_2CSn , the form of the molecular orbitals involved, the molecular orbital occupancies for each state and the electric dipole allowed (solid vertical lines) and forbidden transitions (dashed vertical lines) between the states.

= 13 912 cm⁻¹ (719 nm), which is within the detection range of our CCD/monochromator system.

Our B3LYP DFT results were also used to perform Franck-Condon (FC) simulations of the absorption and single vibronic level (SVL) emission spectra of the various possible electronic transitions as an aid to their detection by laser-induced fluorescence (LIF) and/or emission spectroscopy. The simulation program, originally developed by Yang *et al.*²⁴ and locally modified for the calculation of SVL emission spectra, requires input of the molecular structures, vibrational frequencies and mass-weighted Cartesian displacement coordinates from the *ab initio* force fields of the two combining electronic states. Franck-Condon factors are then calculated in the harmonic approximation using the exact recursion relationships of Doktorov *et al.*²⁵ considering both normal coordinate displacement and Duschinsky rotation effects.

Figure 2 summarizes the results of our *ab initio* studies of the electronic states of H₂C¹²⁰Sn in the form of FC predictions of the $\tilde{B}-\tilde{X}$ absorption spectra and the emission spectra from the lowest vibrational level of the \tilde{B} state down to the ground and first excited singlet states. The absorption (and presumably LIF) spectrum consists of prominent progressions involving ν_3' and ν_2' , due to the calculated 0.04 -0.08 Å increase in the Sn-C bond length and 8-11° increase in the HCH angle on electronic excitation. The $\tilde{B}-\tilde{X}$ emission spectrum is a near-mirror image of the absorption spectrum, with strong bands consisting of combinations of ν_2'' and ν_3'' . In the \tilde{A} state, the Sn-C bond length elongates even further (0.06 – 0.12 Å relative to \tilde{B} state) and the HCH bond angle is similar to that

This is the author's peer reviewed, accepted manuscript. However, the online version of record will be different from this version once it has been copyedited and typeset.
PLEASE CITE THIS ARTICLE AS DOI:10.1063/5.0127449

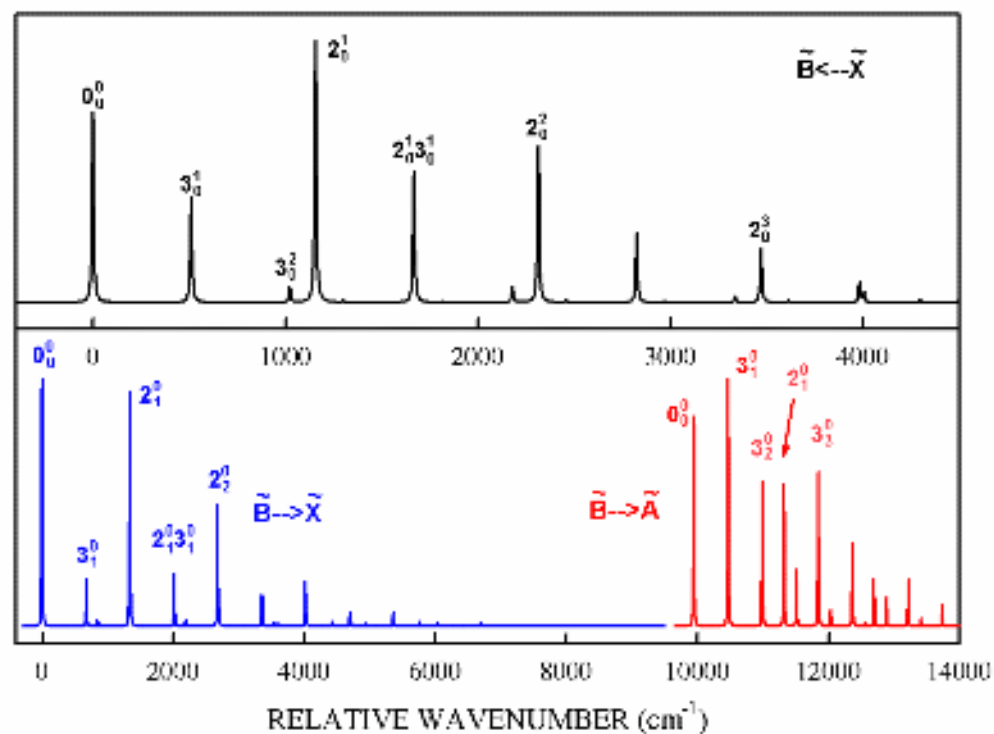


FIG. 2. Franck-Condon simulations of the $^{120}\text{SnCH}_2 \tilde{B} - \tilde{X}$ absorption spectra (top) and $\tilde{B} - \tilde{X}$ and $\tilde{B} - \tilde{A}$ emission spectra (bottom). The absorption spectrum wavenumbers are relative to the 0_0^0 band which our SAC-CI calculations predict to be located at $\sim 23\,928 \text{ cm}^{-1}$. The emission spectra wavenumbers are displacements from the $\tilde{B} - \tilde{X} 0_0^0$ band, giving a direct measure of the lower state vibrational + electronic energy of each vibronic transition. The $\tilde{B} - \tilde{X}$ and $\tilde{B} - \tilde{A}$ emission spectra are separately normalized. The numbering and form of the vibrations is given in Table II.

in the ground state. This leads to a long progression in v_3'' and somewhat weaker activity in v_2'' .

Despite the utility of such simulations, three important caveats must be mentioned. First, these calculations are done in the strictly harmonic approximation, neglecting all anharmonic effects. If the \tilde{A} and \tilde{B} potentials are dissociative or predissociative then the spectra predicated on the absorption or emission of photons will be attenuated relative to the present predictions. Second, in the absence of very substantial changes in the frequencies of the nontotally symmetric vibrations on electronic excitation, the harmonic approximation precludes any involvement of these modes in the spectra. However, vibronic coupling effects can lead to bands involving v_4 , v_5 or v_6 , following the selection rule $\Delta v = \text{odd}$, as we have previously found in the spectra of H_2CSi and H_2CGe . Finally, although the $\tilde{B}-\tilde{A}$ spectra are predicted to have long FC profiles, we recognize, based on our calculations, that the emission from the \tilde{B} state 0^0 level would commence at 719 nm and extend to the red, which is toward the low-energy end of the range of our CCD detector and so may be very weak or undetectable.

IV. RESULTS AND ANALYSIS

A. LIF spectra

Guided by our *ab initio* predictions, we used our 2D LIF spectrometer to search from 20 000 – 25 000 cm^{-1} for LIF signals from the products of a tetramethylstannane/argon discharge. Fig. 3 shows a segment of the resulting spectrum which clearly shows a series of bands from 23 400 24 600 cm^{-1} with similar rotational contours and emission spectra.

This is the author's peer reviewed, accepted manuscript. However, the online version of record will be different from this version once it has been copyedited and typeset.
PLEASE CITE THIS ARTICLE AS DOI:10.1063/5.0127449

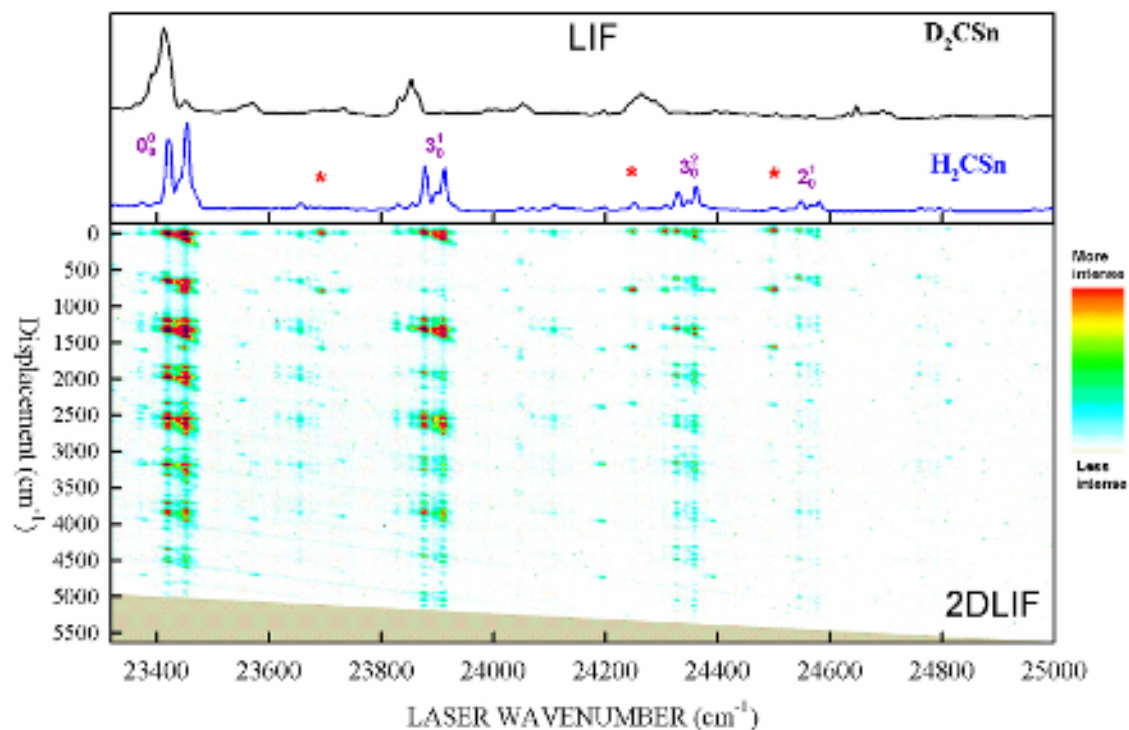


FIG 3. A portion of the 2D LIF spectrum of the discharge products of tetramethylstannane in high pressure argon. The bottom trace in the top panel is the total LIF spectrum, with major features which we assign as due to the H_2CSn molecule. The asterisks denote LIF features due to SnO . The top trace is the LIF spectrum obtained in a separate 2D LIF experiment using a tetramethylstannane- d_{12} precursor. The bottom panel shows the emission spectra recorded at each laser wavenumber in the tetramethylstannane- h_{12} experiment. The ordinate is the emission displacement in cm^{-1} relative to the laser wavenumber.

The technique highlights signals from similar molecules which facilitates the discovery of new species produced in our discharge jet. The top panel show the LIF spectra of D₂CSn (obtained in a separate 2D LIF experiment using tetramethylstannane-d₁₂ as the precursor) and H₂CSn, while the lower panel exhibits the H₂CSn emission spectra versus the laser excitation wavenumber. The emission is given as displacement (laser wavenumber – emission wavenumber, in cm⁻¹), which gives a direct measure of the lower (typically ground state) energy of each transition and is color-coded for intensity. Thus, transitions at 0 cm⁻¹ displacement are resonance fluorescence down to the initial vibrational level from which laser excitation took place and a transition with a displacement of 500 cm⁻¹ would be a transition from the upper vibronic state populated by the laser to an energy level 500 cm⁻¹ above the initial vibrational level.

In addition to readily identified bands of SnO,²⁶ with a vibrational interval of ~800 cm⁻¹, the 2D LIF spectrum in Fig. 3 exhibits a series of weak features with similar rotational contours and emission spectra, starting with a band centered at ~23 430 cm⁻¹. The bands have the partially resolved rotational contour expected for an asymmetric top with an *A* value of ~10 cm⁻¹, as must be the case for planar H₂CSn. Prominent emission intervals of ~650 and ~1340 cm⁻¹ are readily ascribed to the FC active Sn-C stretch and CH₂ symmetric stretch (see Table II). The D₂CSn LIF spectrum is similar to that from TMSn, but the bands exhibit a different rotational contour and are slightly red shifted, precisely as predicted by our *ab initio* calculations (Table II).

In the discussion that follows, we denote comparisons of band origins or vibrational frequencies for the two isotopologues as H₂CSn/D₂CSn and compare calculated *ab initio*

frequencies of a single isotopologues as CCSD(T)(B3LYP), following the convention in Table II.

Fig. 4 shows the first bands in the spectra of H₂CSn and D₂CSn at somewhat higher resolution (~ 0.1 cm⁻¹), recorded with the Lumonics dye laser. The upward-going traces are the experimental data and the downward traces are the calculated band profiles of the ¹²⁰Sn isotopologue, with the rotational constants taken from the *ab initio* geometries (Table II). Each exhibits the typical rotational contour of a perpendicular band (in this case, bands following *b*-type selection rules) of an asymmetric top. We assign these bands as 0_0^0 and the estimated band origins [23 430.4/23 406.3 cm⁻¹] compare favorably with the *ab initio* SAC-CI values of [23 928/23 895 cm⁻¹] from Table II. For a ground state of A₁ symmetry, the nuclear statistical weights of H₂CSn vary according to the even (e) or odd (o) values of K_a , K_c as e,e = e,o = 1; o,o = o,e = 3 so the central rQ_0 branch would be expected to be abnormally weak, as is observed. Deuterium substitution changes the nuclear statistical weights so that e,e = e,o = 2; o,o = o,e = 1, giving greater intensity to rQ_0 , precisely as observed. The correspondence of the observed and calculated band contours and transition energies leaves little doubt that the spectra are those of the $\tilde{B}^1B_2 - \tilde{X}^1A_1$ band system of the previously spectroscopically unobserved stannylidene molecule.

In accord with the calculated FC absorption spectrum profile (Fig. 2) and the *ab initio* excited state frequencies (Table II), we assign the remaining H₂CSn LIF bands (Fig. 3) as 3_0^1 , 3_0^2 , 2_0^1 with a possible weak 3_0^3 band at the blue end as summarized in Table III. These assignments give $\nu_3' = 458.6$ cm⁻¹ [*ab initio* = 580(511)] and $\nu_2' = 1128.7$ cm⁻¹ [*ab*

This is the author's peer reviewed, accepted manuscript. However, the online version of record will be different from this version once it has been copyedited and typeset.
PLEASE CITE THIS ARTICLE AS DOI:10.1063/5.0127449

initio = 1166(1157)]. The D₂CSn LIF spectrum was weaker and only the 3₀¹, 3₀² and 2₀¹ bands were assignable, giving $\nu_3' = 442.6 \text{ cm}^{-1}$ [*ab initio* = 555(485)] and $\nu_2' = 854.4 \text{ cm}^{-1}$

This is the author's peer reviewed, accepted manuscript. However, the online version of record will be different from this version once it has been copyedited and typeset.
PLEASE CITE THIS ARTICLE AS DOI:10.1063/5.0127449

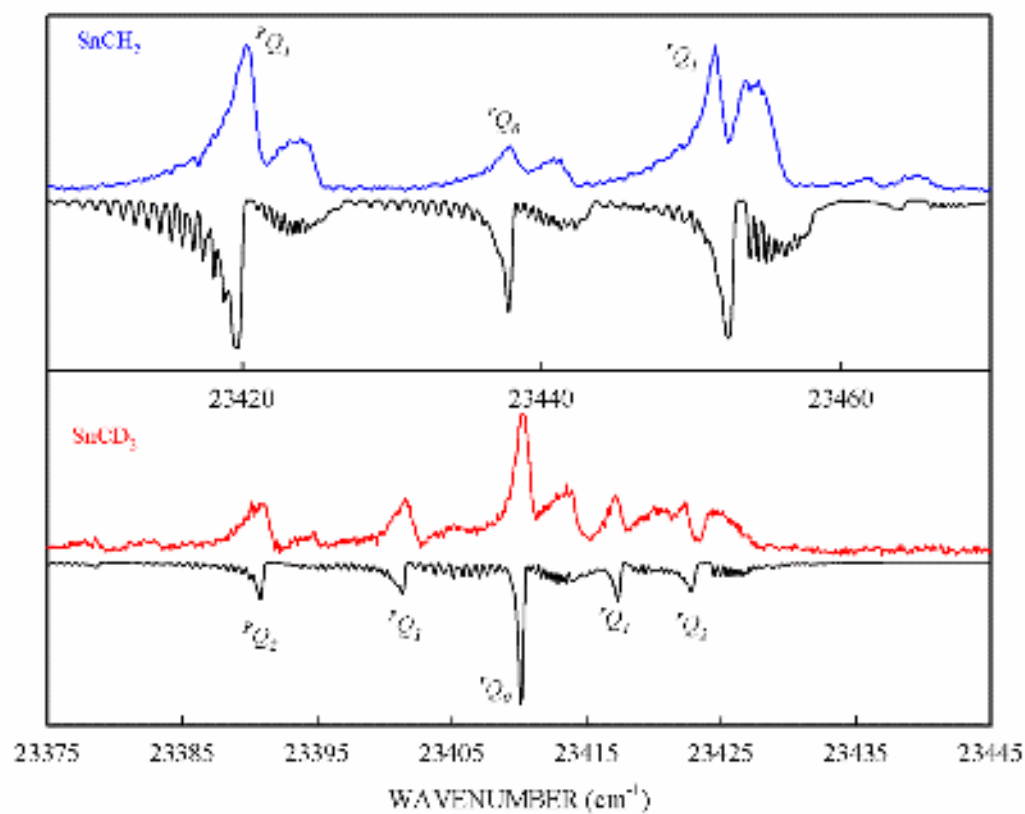


FIG. 4. Low-resolution LIF spectra (upward going features) of the 0-0 bands of H_2CSn (top) and D_2CSn (bottom) along with simulations (downward going features) of the spectra based on the rotational constants derived from the B3LYP geometries in Table II, a linewidth of 0.25 cm^{-1} and a rotational temperature of 30 K.

TABLE III. Assignments and approximate band origins (cm^{-1}) of the observed bands in the LIF spectra of H_2CSn and D_2CSn .

Assign.	H_2CSn			D_2CSn		
	T_0	Comment ^a	<i>Ab Initio</i> ^b	T_0	Comment ^c	<i>Ab Initio</i> ^b
0_0^0	23430.4		$T_0 = 23928$	23406.3	H/D shift = -24.1	H/D shift = -33 $T_0 = 23895$
3_0^1	23889.0	+458.6	$\overset{\cdot}{\nu}_3 =$ 580(511)	23848.9	+442.6 H/D shift = -16.0	$\overset{\cdot}{\nu}_3 =$ 555(485) H/D shift = -25(-26)
3_0^2	24338.6	+908.2 $3_0^1 +$ 449.6		24283.0?	+876.7 $3_0^1 + 434.1$	
2_0^1	20559.1	+1128.7	$\overset{\cdot}{\nu}_2 =$ 1166(1157)	24260.7?	+854.4 H/D shift = -274.3	$\overset{\cdot}{\nu}_2 =$ 856(858) H/D shift = -310(299)
3_0^3	24771.5?	+1341.1 $3_0^2 +$ 432.9				

^aFor H_2CSn , T_0 calculated as pQ_I maximum + $(A - \bar{B})'' = 9.9 \text{ cm}^{-1}$ from B3LYP geometry.

^bSee Table II, SAC-CI results.

^cFor D_2CSn , T_0 calculated as rQ_0 maximum - $(A - \bar{B})' = 4.0 \text{ cm}^{-1}$ from B3LYP geometry.

This is the author's peer reviewed, accepted manuscript. However, the online version of record will be different from this version once it has been copyedited and typeset.
PLEASE CITE THIS ARTICLE AS DOI:10.1063/5.0127449

[*ab initio* = 856(858)]. In both isotopologues, ν_2' is in good accord with experiment but theory overestimates the ν_3' frequency to be $\text{H}_2\text{CSn} = 121.4/52.4 \text{ cm}^{-1}$ and $\text{D}_2\text{CSn} = 112.4/42.4 \text{ cm}^{-1}$ larger than experiment. Alternative assignments involving the nontotally symmetric modes were considered but rejected as the frequency mismatch is even greater.

B. Emission spectra

Although the LIF spectra of stannylidene proved to be weak and of limited extent, the emission spectra were much more informative. Fig. 5 shows the emission bands observed following laser excitation of the strong pQ_1 branch of the 0-0 band of H_2CSn . The main $\tilde{B} - \tilde{X}$ band system extends approximately $6\,500 - 7\,000 \text{ cm}^{-1}$ to the red of the excitation laser, precisely as predicted by our FC calculations (see Fig. 2). Of particular note is the occurrence of an additional weak band system, assigned as $\tilde{B}^1\text{B}_2 - \tilde{A}^1\text{A}_2$, at a displacement of $\sim 9\,800 \text{ cm}^{-1}$, similar to that observed in the $\tilde{B}^1\text{B}_2$ state emission spectrum of H_2CGe .⁹ Deuteration shifts the bands in the long wavelength system slightly, as shown in the inset in Fig. 5. In each case, the band system consists of only two bands, which we assign as 0_0^0 and 3_1^0 , based on our FC predictions (Fig 2). and the measured \tilde{A} state ν_3 intervals of $\text{H}_2\text{CSn}/\text{D}_2\text{CSn} = 519/487 \text{ cm}^{-1}$, in complete accord with calculated values of $\text{CCSD(T)} = 542/505$ and $\text{B3LYP} = (522/487) \text{ cm}^{-1}$. The measured displacements give \tilde{A} state T_0 values of $9\,828/9\,783 \text{ cm}^{-1}$ which can be compared to our best *ab initio* SAC-CI values of $10\,016/10\,004 \text{ cm}^{-1}$. Although the FC calculations predict a rather extensive $\tilde{B} - \tilde{A}$ band system (Fig. 2), we were fortunate to catch the very edge of the emission spectrum at $730 - 760 \text{ nm}$ as the detection efficiency of our CCD/monochromator detection system

This is the author's peer reviewed, accepted manuscript. However, the online version of record will be different from this version once it has been copyedited and typeset.
PLEASE CITE THIS ARTICLE AS DOI:10.1063/5.0127449

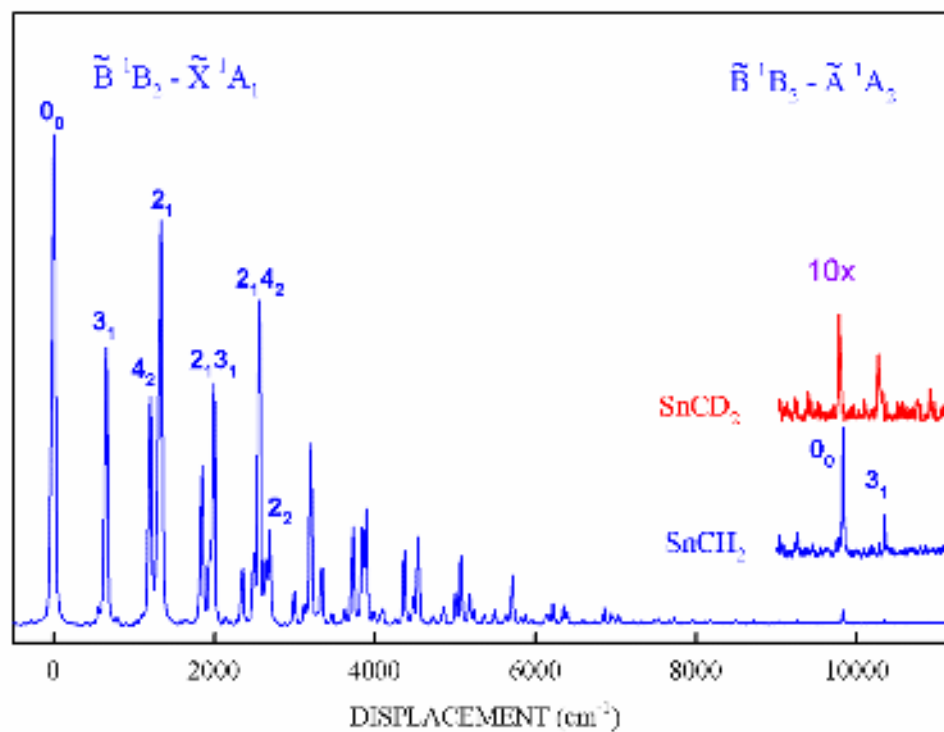


FIG. 5. Low-resolution emission spectrum obtained by laser excitation of the 0-0 band pQ_1 branch of the LIF spectrum of H₂CSn. This spectrum was recorded using a low-resolution 300 line/mm diffraction grating blazed at 500 nm.

decreases markedly in this region.

The $\tilde{B} - \tilde{X}$ emission bands of both isotopologues were assigned based on the FC calculations, *ab initio* frequencies and comparisons to the analogous spectra of H₂CSi and H₂CGe.^{6,7} Our highest resolution emission spectra of H₂CSn are compared in Fig. 6. The first H₂CSn strong band, with an interval of 653 cm⁻¹ [B3LYP = 678], is clearly 3₁⁰. The next strong band, at 1198 cm⁻¹, must be assigned as 4₂⁰, just as it was for H₂CSi and H₂CGe, giving $\nu_4'' = 599$ [B3LYP = 648]. As predicted by the FC calculations, the next strong feature in both spectra is 2₁⁰ with $\nu_2'' = 1339$ cm⁻¹ [B3LYP = 1340 cm⁻¹]. The majority of the subsequent bands in the 0-0 band spectrum can be assigned as overtones or combinations of the ν_2 , ν_3 and ν_4 fundamentals, as summarized in Table IV. The near degeneracy of 2_{1,32} and 4₂ often led to multiple possible assignments of the higher energy bands, so these should be regarded as tentative.

We also recorded emission spectra from some of the vibrationally excited levels in the \tilde{B} states of H₂CSn. Although the 2₀¹ band spectrum did not provide any new information, the 3₀¹ and 3₀² band emission spectra (see Fig. 6) both exhibited weak features which could be assigned as transitions down to the 6₂ and 2_{1,62} levels, giving $\nu_6'' = 399$ cm⁻¹ [B3LYP = 426 cm⁻¹]. The observed activity in ν_6'' is markedly less than that found in the spectra of silylidene or germylidene.^{6,7}

The emission spectra of D₂CSn were less extensive, primarily due to a dearth of the TMSn-d₁₂ precursor, yielding only spectra from pQ_1 excitation of the 0₀⁰ and 3₀¹ bands, as

This is the author's peer reviewed, accepted manuscript. However, the online version of record will be different from this version once it has been copyedited and typeset.
PLEASE CITE THIS ARTICLE AS DOI:10.1063/5.0127449

shown in Fig. 7. In this case, transitions to $v_3'' = 588 \text{ cm}^{-1}$ [B3LYP = 621 cm^{-1}] are quite weak, but the 2_1 and 4_2 levels show up very strongly as they are in Fermi resonance and their perturbed separation is only 67 cm^{-1} . The transition to 2_1 is expected to be prominent on Franck-Condon grounds but to zero-order the transition to 4_2 would be expected to have negligible intensity. The Fermi resonance dilutes the oscillator strength of emission to 2_1 , sharing it with the 4_2 level. The 3_0^1 emission spectrum show extra features which can be ascribed to activity in $2v_6''$ giving $v_6'' = 310 \text{ cm}^{-1}$ [B3LYP = 320 cm^{-1}]. Previously, we identified the symmetric CH stretching interval in the emission spectra of $\text{D}_2\text{CSi} = 2185 \text{ cm}^{-1}$ and $\text{D}_2\text{CGe} = 2089 \text{ cm}^{-1}$ and there is fragmentary evidence of a $3_0^1 1_1^0$ band which appears as a shoulder at 1980 cm^{-1} [B3LYP = 2235 cm^{-1}] on the stronger $3_0^1 2_1^0 4_2^0$ band. The D_2CSn emission spectra proved quite difficult to assign as the intervals among the lower energy strong bands were irregular, presumably due to $v_2/2v_4$ Fermi resonance effects. Our best efforts at assignments, which may need revision if more extensive data becomes available, are given in Table IV.

This is the author's peer reviewed, accepted manuscript. However, the online version of record will be different from this version once it has been copyedited and typeset.
PLEASE CITE THIS ARTICLE AS DOI:10.1063/5.0127449

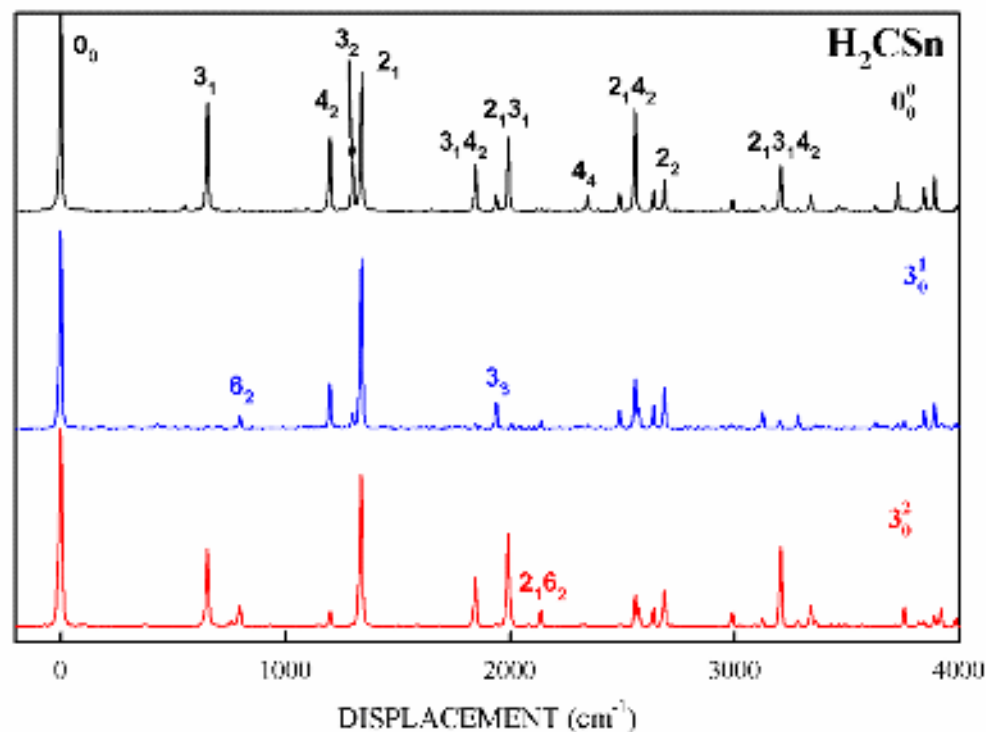


FIG. 6. Comparison of the $\tilde{B}^1B_2 - \tilde{X}^1A_1$ emission spectra obtain by laser excitation of the pQ_1 branch of the 0_0^0 , 3_0^1 and 3_0^2 LIF bands of H_2CSn . The horizontal scale is the wavenumber displacement of the emission from the excitation laser wavenumber which gives a direct measure of the vibrational energy in the lower state.

This is the author's peer reviewed, accepted manuscript. However, the online version of record will be different from this version once it has been copyedited and typeset.
PLEASE CITE THIS ARTICLE AS DOI:10.1063/5.0127449

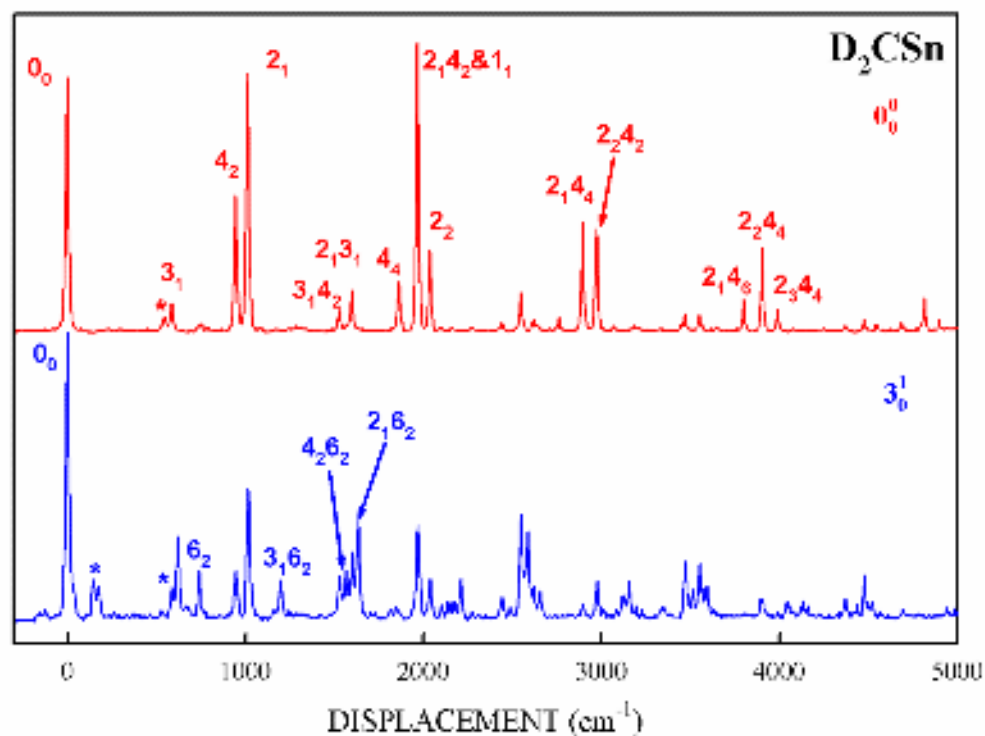


FIG. 7. Comparison of the $\tilde{B}^1B_2 - \tilde{X}^1A_1$ emission spectra obtain by laser excitation of the pQ_1 branch of the 0_0^0 and 3_0^1 LIF bands of D_2CSn . The horizontal scale is the wavenumber displacement of the emission from the excitation laser wavenumber which gives a direct measure of the vibrational energy in the lower state. Asterisks denote impurity transitions.

Table IV. Summary of the lower state vibrational levels of H₂CSn and D₂CSn measured from single vibronic level emission spectra.

H ₂ CSn			D ₂ CSn		
Energy (cm ⁻¹)	Assign.	Comment	Energy (cm ⁻¹)	Assign.	Comment
653	3 ₁	v ₃ = 653	588	3 ₁	v ₃ = 588
798	6 ₂	v ₆ = 399	620	6 ₂	v ₆ = 310
1198	4 ₂	v ₄ = 599	945	4 ₂	v ₄ = 473
1299	3 ₂	3 ₁ + 646	1012	2 ₁	v ₂ = 1012
1339	2 ₁	v ₂ = 1339	1199	3 ₁ 6 ₂	6 ₂ + 579
1846	3 ₁ 4 ₂	4 ₂ + 648	1527	3 ₁ 4 ₂	4 ₂ + 582
1938	3 ₃	3 ₂ + 639	1565	4 ₂ 6 ₂	4 ₂ + 620
1993	2 ₁ 3 ₁	2 ₁ + 654	1597	2 ₁ 3 ₁	2 ₁ + 585
2009	4 ₂ 6 ₂	4 ₂ + 811	1634	2 ₁ 6 ₂	2 ₁ + 621.2
2137	2 ₁ 6 ₂	2 ₁ + 798	1861	4 ₄	4 ₂ + 916
2346	4 ₄	4 ₂ + 1148	1969	2 ₁ 4 ₂	4 ₂ + 1024
2488	3 ₂ 4 ₂	3 ₁ 4 ₂ + 641.4	1980	1 ₁ ?	4 ₂ + 1051
2557	2 ₁ 4 ₂	2 ₁ + 1218	2036	2 ₂	2 ₁ + 1024
2572	3 ₄	3 ₃ + 634	2102	3 ₂ 4 ₂	3 ₁ 4 ₂ + 575
2639	2 ₁ 3 ₂	2 ₁ 3 ₁ + 646	2139	3 ₁ 4 ₂ 6 ₂	4 ₂ 6 ₂ + 574
2688	2 ₂	2 ₁ + 1349	2170	2 ₁ 3 ₂	2 ₁ 3 ₁ + 573
2991	3 ₁ 4 ₄	4 ₄ + 645	2210	2 ₁ 3 ₁ 6 ₂	2 ₁ 6 ₂ + 576
3125	3 ₃ 4 ₂	3 ₂ 4 ₂ + 637	2439	3 ₁ 4 ₄	4 ₄ + 578
3201	2 ₁ 3 ₁ 4 ₂	2 ₁ 4 ₂ + 644	2546	2 ₁ 3 ₁ 4 ₂	2 ₁ 4 ₂ + 577
3281	2 ₁ 3 ₃	2 ₁ 3 ₂ + 642	2586	2 ₁ 4 ₂ 6 ₂	2 ₁ 4 ₂ + 590
3338	2 ₂ 3 ₁	2 ₂ + 650	2617	2 ₂ 3 ₁	2 ₂ + 581
3363	2 ₁ 4 ₂ 6 ₂	4 ₂ 6 ₂ + 1354	2656	2 ₂ 6 ₂	2 ₁ 6 ₂ + 1022
3462	4 ₆	4 ₄ + 1116	2761	4 ₆ ?	4 ₄ + 900
3629	3 ₂ 4 ₄	3 ₁ 4 ₄ + 638	2893	2 ₁ 4 ₄	4 ₄ + 1032
3726	2 ₁ 4 ₄	4 ₄ + 1380	2972	2 ₂ 4 ₂	2 ₁ 4 ₂ + 1003
3755	3 ₄ 4 ₂	3 ₃ 4 ₂ + 630	3013	3 ₂ 4 ₄	3 ₁ 4 ₄ + 574
3844	2 ₁ 3 ₂ 4 ₂	2 ₁ 3 ₁ 4 ₂ + 643	3155	1 ₁ 3 ₁ 6 ₂ ?	1 ₁ 3 ₁ + 609
3890	2 ₂ 4 ₂ ?	2 ₁ 4 ₂ + 1333	3469	2 ₁ 3 ₁ 4 ₄	2 ₁ 4 ₄ + 576
3918	2 ₁ 3 ₄	2 ₁ 3 ₃ + 637	3516	2 ₁ 4 ₄ 6 ₂	2 ₁ 4 ₄ + 623
3985	2 ₂ 3 ₂	2 ₂ 3 ₁ + 647	3551	2 ₂ 3 ₁ 4 ₂	2 ₂ 4 ₂ + 579
4067	2 ₁ 3 ₃ 6 ₂	?	3594	2 ₂ 4 ₂ 6 ₂	2 ₂ 4 ₂ + 622
4261	3 ₃ 4 ₄	3 ₂ 4 ₄ + 632	3798	2 ₁ 4 ₆	4 ₆ + 1037
4369	2 ₁ 3 ₁ 4 ₄	2 ₁ 4 ₄ + 643	3902	2 ₂ 4 ₄	2 ₁ 4 ₄ + 1009
4377	3 ₅ 4 ₂	3 ₄ 4 ₂ + 622	3989	2 ₃ 4 ₂	2 ₂ 4 ₂ + 1017
4442	3 ₂ 4 ₄ 6 ₂	?	4369	2 ₁ 3 ₁ 4 ₆	2 ₁ 4 ₆ + 571
4479	2 ₁ 3 ₃ 4 ₂	2 ₁ 3 ₂ 4 ₂ + 635	4476	2 ₂ 3 ₁ 4 ₄	2 ₂ 4 ₄ + 574
4538	2 ₁ 3 ₅	2 ₁ 3 ₄ + 620	4542	2 ₃ 3 ₁ 4 ₂	2 ₃ 4 ₂ + 553
4855	2 ₁ 4 ₆	4 ₆ + 1393	4686	2 ₁ 4 ₈ ?	2 ₁ 4 ₆ + 888
4887	3 ₄ 4 ₄	3 ₃ 4 ₄ + 626	4816	2 ₂ 4 ₆	2 ₁ 4 ₆ + 1018
5008	2 ₁ 3 ₂ 4 ₄	2 ₁ 3 ₁ 4 ₄ + 638	4898	2 ₃ 4 ₄	2 ₂ 4 ₄ + 996

This is the author's peer reviewed, accepted manuscript. However, the online version of record will be different from this version once it has been copyedited and typeset.
PLEASE CITE THIS ARTICLE AS DOI:10.1063/5.0127449

This is the author's peer reviewed, accepted manuscript. However, the online version of record will be different from this version once it has been copyedited and typeset.
PLEASE CITE THIS ARTICLE AS DOI:10.1063/1.50127449

5073	3 ₃ 4 ₄ 6 ₂	3 ₂ 4 ₄ 6 ₂ + 631
5104	2 ₁ 3 ₄ 4 ₂	2 ₁ 3 ₃ 4 ₂ + 625
5178	3 ₅ 4 ₂ 6 ₂ ?	3 ₅ 4 ₂ + 801
5265	2 ₂ 3 ₄	2 ₁ 3 ₄ + 1347
5508	3 ₅ 4 ₄	3 ₄ 4 ₄ + 621
5637	2 ₁ 3 ₃ 4 ₄	2 ₁ 3 ₂ 4 ₄ + 629
5725	2 ₁ 3 ₅ 4 ₂	2 ₁ 3 ₄ 4 ₂ + 621
6260	2 ₁ 3 ₄ 4 ₄	2 ₁ 3 ₃ 4 ₄ + 623
6441	2 ₁ 3 ₃ 4 ₄ 6 ₂	?

9828	0 ₀	$\tilde{\text{A}}$ state	9783	0 ₀	$\tilde{\text{A}}$ state
10347	3 ₁	$v_3 = 519.0$	10270	3 ₁	$v_3 = 487$

V. DISCUSSION

A. Molecular structures

With ten naturally occurring tin isotopes, rotational analysis of the $\tilde{B} - \tilde{X}$ 0-0 bands of H_2CSn and D_2CSn is not possible with our current resources, so we must rely on the results of our *ab initio* calculations for structural information. Table V summarizes the results from the present work and compares them with experimental values for H_2CSi and H_2CGe . The ground state C-Sn bond length of 2.000 Å is comparable to the 2.003 Å C=Sn bond length in bis(2,4,6-triisopropylphenyl)-2,7-di-tert-butylfluorenylidene stannane²⁷ determined by X-ray crystallography and is considerably shorter than typical carbon-tin single bonds (2.15 – 2.16 Å).²⁸ The methylene group geometric parameters are largely invariant to substitution by Si, Ge or Sn with average values of $r(\text{CH}) = 1.097$ Å and $\theta(\text{HCH}) = 114.5^\circ$. The bond length of free methylene²⁹ ($\text{CH}_2 \tilde{X}^3\text{A}_1$) is 1.075 Å and the bond angle is 133.8° , illustrating that attaching the heteroatom closes the bond angle substantially and very slightly elongates the CH bond. Similar results are found for formaldehyde [$r_z(\text{CH}) = 1.100$ Å, $\theta_z(\text{HCH}) = 116.23^\circ$], thioformaldehyde [$r_z(\text{CH}) = 1.096$ Å, $\theta_z(\text{HCH}) = 116.27^\circ$]³⁰ and selenoformaldehyde [$r_s(\text{CH}) = 1.090$ Å, $\theta_s(\text{HCH}) = 117.9^\circ$]³¹, indicating that the CH bond length is largely invariant but that the bond angle has a small dependence on the identity of the heteroatom.

Promotion of an electron from the π bonding HOMO to the LUMO, an in-plane nonbonding $5p$ orbital on the tin atom, yields low-lying $\tilde{a}^3\text{A}_2$ and $\tilde{A}^1\text{A}_2$ excited states in which there is a substantial elongation of the C-Sn bond (0.15 Å) and only minor changes to the CH_2 geometry relative to the ground state. The data in Table V shows precisely the

TABLE V. Comparison of the ground state molecular structures and structural changes on electronic excitation for H₂CX (X = Si, Ge, Sn) molecules.

\tilde{X}^1A_1 Ground State					
	$r(\text{C-X}) \text{ \AA}$	$r(\text{C-H}) \text{ \AA}$	$\theta(\text{HCH})^\circ$	T_0	Source
H₂CSi	1.706	1.099	114.4	0	Expt. Ref. 4
H₂CGe	1.791	1.102	115.1	0	Expt. Ref. 5
H₂CSn	2.000	1.090	114.0	0	SAC-CI This work
\tilde{A}^1A_2 Excited State					
	$\Delta r(\text{C-X}) \text{ \AA}$	$\Delta r(\text{C-H}) \text{ \AA}$	$\Delta\theta(\text{HCH})^\circ$	T_0	Source
H₂CSi	0.167	0.0	-0.5	15 132.966	Expt. Ref. 8
H₂CGe	0.167	0.0 ^a	-3.7	13 263.095	Expt. Ref. 9
H₂CSn	0.15	-0.020	-2.1	9 782.7 ^b	SAC-CI This work
\tilde{B}^1B_2 Excited State					
	$\Delta r(\text{C-X}) \text{ \AA}$	$\Delta r(\text{C-H}) \text{ \AA}$	$\Delta\theta(\text{HCH})^\circ$	T_0	Source
H₂CSi	0.109	-0.026	19.3	29 312.875	Expt. Ref. 4
H₂CGe	0.123	-0.020	24.3	27 330.423	Expt. Ref. 5
H₂CSn	0.084	-0.014	20.4	23 430.4 ^c	SAC-CI This work

^aFixed at ground state value.

^bExpt. value from Table IV.

^cExpt. value from Table III.

This is the author's peer reviewed, accepted manuscript. However, the online version of record will be different from this version once it has been copyedited and typeset.
PLEASE CITE THIS ARTICLE AS DOI:10.1063/5.0127449

same effects in the \tilde{A} states of H₂CSi and H₂CGe, as derived from rotational analyses of experimental spectra.

The \tilde{B}^1B_2 state is formed by promotion of an electron from the second highest occupied molecular orbital (SHOMO), a C-Sn σ bonding orbital which is also bonding between the two hydrogens (see Fig. 1), to the aforementioned nonbonding LUMO orbital. This has the effect of elongating the C-Sn bond (0.084 Å) and substantially increasing the HCH angle (+20.4°). Again, the experimentally derived results for silylidene and germylidene show exactly these types of changes, lending confidence to our stannylidene *ab initio* results.

The good agreement between the experimental and simulated stannylidene $\tilde{B} - \tilde{X}$ 0-0 band rotational contours (see Fig. 4) provides evidence that the calculated molecular geometries from which the contours are derived cannot be substantially in error. Similarly, the satisfactory correspondence between the observed and calculated ground state vibrational frequencies of both isotopologues argues for the validity of the *ab initio* results.

B. Electronic transitions

Experiment gives stannylidene T_0 values of $\tilde{B} - \tilde{X} = 23\,430.4/23\,406.2$ cm⁻¹ and $\tilde{A} - \tilde{X} = 9\,828/9\,783$ cm⁻¹. SAC-CI theory predicts the corresponding values as 23 928/23 895 cm⁻¹ and 10 016/10 004 cm⁻¹, which is excellent agreement, with a maximum error of 2.1% and the signs of the observed deuterium isotope shifts are as expected. The differences between magnitudes of the calculated and experimentally measured isotope shifts are undoubtedly due to the neglect of anharmonicity in the *ab initio* values. The experimentally determined energies of the \tilde{A} and \tilde{B} excited states of silylidene, germylidene and

stannylidene are compared in Table V, which shows a monotonic decrease in both states as a function of the atomic number of the heteroatom.

The LIF spectra of H₂CSn and D₂CSn are very weak and much less extensive than expected (based on similar spectra of H₂CSi and H₂CGe), which probably accounts for our failure to observe the bands in our early work.² Our experience also shows that, depending on the experimental conditions, the LIF spectra of Sn₂ and SnO can be very strong in this region and they may have overwhelmed the weaker H₂CSn spectra. It is unfortunate that the stannylidene LIF spectra contain so few bands as they provide little information on the excited state. We speculate that the H₂CSn \tilde{B} state has a shallow potential well and is dissociative or predissociated, which makes LIF spectroscopy challenging.

C. Vibronic structure

The \tilde{X} and \tilde{A} state vibrational frequencies of H₂CSn and D₂CSn are quite reliably predicted by CCSD(T) and B3LYP methods using the triple zeta basis sets employed in the present work. The situation is less satisfactory for the \tilde{B} state, where somewhat larger discrepancies were noted between the observed and calculated C-Sn stretching frequencies, which may be a sign of the excited state dissociation alluded to previously.

Of most interest is the fact that transitions involving ν_4'' and ν_6'' appear in the $\tilde{B} - \tilde{X}$ emission spectra of stannylidene, as they do in the spectra of silylidene and germylidene, but it is clear that the ν_6 activity is much less pronounced in the tin-containing molecule. In fact, the ground state CH₂ rocking mode (ν_6) in all these molecules is rather peculiar. The ν_6'' frequencies are silylidene = 263/210, germylidene = 351/282 and stannylidene = 398/310 cm⁻¹, much smaller than expected and contrary to the usual trend of decreasing

frequency with heavier heteroatom. For example, the experimental ν_6'' frequencies of the formaldehyde-type molecules^{30,32} are $\text{H}_2\text{CO} = 1249$, $\text{H}_2\text{CS} = 991$ and $\text{H}_2\text{CSe} = 913 \text{ cm}^{-1}$. In contrast, it is noteworthy that the expected trend *is followed* in the $\tilde{B}^1\text{B}_2$ excited states with $\nu_6' = 731/548 \text{ cm}^{-1}$ for silylidene and $692/513 \text{ cm}^{-1}$ for germylidene, with frequencies more consistent with those of the formaldehyde-type molecules.

Previously⁷, we proposed a simple model based on the ground state *ab initio* H_2CX to trans-bent HXCH isomerization transition state energies to rationalize these observations, as shown in Fig. 8. The transition states all have similar geometries and have energies relative to the bottom of the ground state potential of $\text{H}_2\text{CSi} = 38.5$, $\text{H}_2\text{CGe} = 52.0$ and $\text{H}_2\text{CSn} = 60.1 \text{ kcal/mol}$. [CCSD(T) calculations from refs. 10, 34 and the present work]. The CH_2 rocking vibration serves as a promoting mode for the isomerization which occurs along the Q_6 normal coordinate and, for simplicity, we model the potential as harmonic. With similar transition state structures, we make the assumption that it takes approximately the same displacement along the Q_6 normal coordinate to reach the transition state in each case. As is obvious from the figure, higher energy transition states lead to steeper potentials and larger ν_6 frequencies, in accord with experiment. The observed spectroscopic activity in ν_6 can then be understood, at least in part, based on the large difference in the frequencies in the \tilde{B} and \tilde{X} states.

The activity in ν_4 is more difficult to explain, as the out-of-plane bending frequencies of all the H_2CX molecules are similar in the \tilde{X} and \tilde{B} states, with ν_4''/ν_4' values of $\text{H}_2\text{CSi} = 687/697$, $\text{H}_2\text{CGe} = 672/613$ and $\text{H}_2\text{CSn} = 599/629$ (ν_4' from theory, Table II).

This is the author's peer reviewed, accepted manuscript. However, the online version of record will be different from this version once it has been copyedited and typeset.
PLEASE CITE THIS ARTICLE AS DOI:10.1063/5.0127449

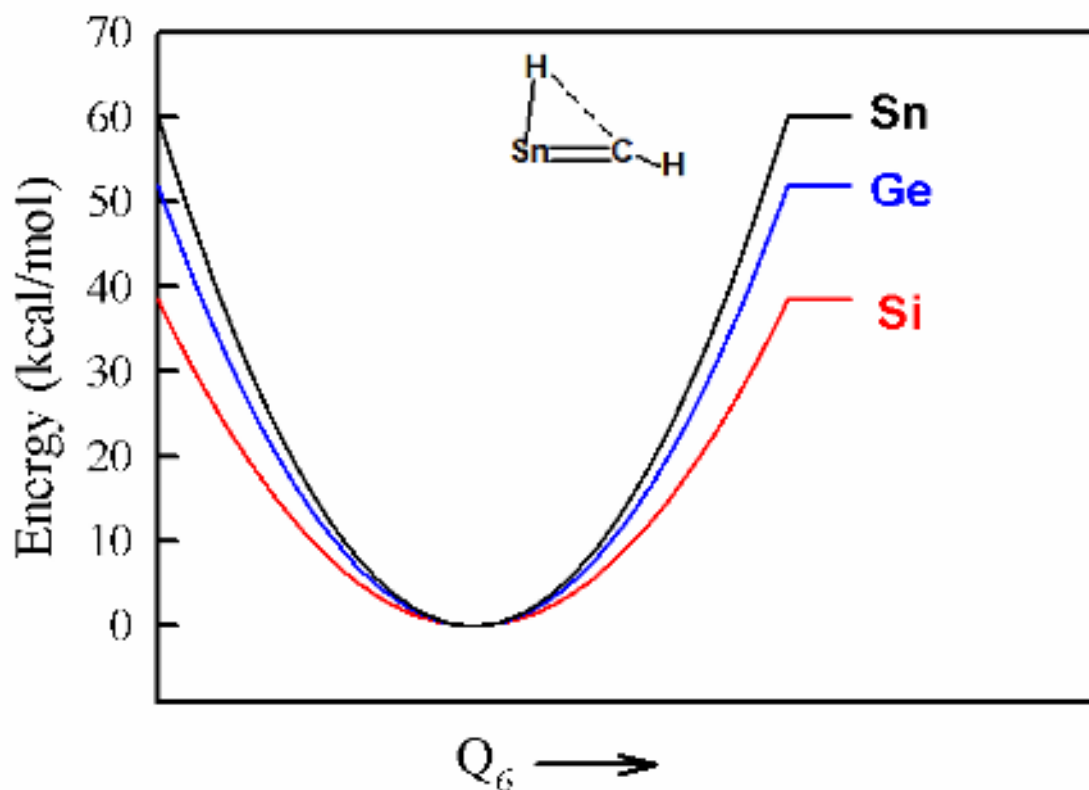


FIG. 8. Schematic diagram of harmonic potentials along the ν_6'' (CH_2 rocking) normal coordinate of H_2CX ($\text{X} = \text{Si}, \text{Ge}$ and Sn) vs the energies of the transition states for the isomerization to the trans-bent acetylenic isomer. The structure of the H_2CSn transition state found in this work [CCSD(T) method] is given. The transition state energies are 38.5, 52.0 and 61.0 kcal/mol above the bottom of the potential.^{10,33}

This is the author's peer reviewed, accepted manuscript. However, the online version of record will be different from this version once it has been copyedited and typeset.
PLEASE CITE THIS ARTICLE AS DOI:10.1063/5.0127449

It is tempting to ascribe the activity in even quanta of ν_4 to the ν_2 - $2\nu_4$ Fermi resonance, but the data preclude such a facile explanation. For example, the 0-0 band emission spectrum of H₂CGe shows a transition to 4_2 which is about 20% stronger than that to 2_1 . In the event that the unperturbed separation of 4_2 and 2_1 is almost zero, one would expect at most a 50-50 mixing and equal sharing of the intensity between the 2_1^0 and 4_2^0 bands. In D₂CGe, 4_2 and 2_1 are actually measured to be in closer proximity (38 cm⁻¹ vs 107 cm⁻¹ in H₂CGe), but 4_2^0 is ~20% weaker than 2_1^0 . In the present work, the 0-0 band emission spectra show $4_2^0:2_1^0$ intensity ratios of approx.. 1:2 in H₂CSn and D₂CSn, despite the levels being significantly closer together (67 vs 141 cm⁻¹) in D₂CSn. Similarly, the 4_0^2 and 2_0^1 bands are evident in the LIF spectra of H₂Si and D₂CSi, despite the fact that the upper state levels are 291 and 263.4 cm⁻¹ apart, respectively, and appear with similar intensities in the LIF spectra of H₂CGe and D₂CGe, with upper state separations of 202.6 and 147.4 cm⁻¹. A purely Fermi resonance explanation simply cannot accommodate all these disparate experimental facts.

In our analysis of the LIF spectra of silylidene and germylidene, evidence was presented that the upper state out-of-plane bending potentials of both molecules are quite anharmonic, with level separations that increase rather than decrease with the ν_4 quantum number.⁷ Unfortunately, similar data is not available for H₂CSn and D₂CSn, due to the limited extent of the LIF spectra. A consequence of the large anharmonicity is that levels of the same vibronic symmetry can mix and the transition intensity is shared between them, accounting in a qualitative fashion for the anomalous intensities in the LIF and emission spectra. A similar effect is found in the S₁ - S₀ spectra of 2-pyradone, which show activity in even quanta of the out-of-plane bending modes, associated anharmonic potentials and a

This is the author's peer reviewed, accepted manuscript. However, the online version of record will be different from this version once it has been copyedited and typeset.
PLEASE CITE THIS ARTICLE AS DOI:10.1063/5.0127449

slight nonplanarity in the excited state.³⁴ A quantitative description of the ν_4 activity in the spectra of silylidene, germylidene and stannylidene awaits further experimental and/or theoretical studies.

VI. CONCLUSIONS

Stannylidene (H_2CSn and D_2CSn) has been identified in the gas phase for the first time by observation of the $\tilde{B}^1\text{B}_2 - \tilde{X}^1\text{A}_1$ LIF transition of the jet-cooled molecules. The correspondence between our *ab initio* predictions and the experimentally observed electronic band origins, 0-0 band rotational contours, vibrational frequencies, FC profiles of the spectra and H/D isotope shifts provides incontrovertible evidence for the discovery. These studies show that the spectroscopy of stannylidene is, in many ways, analogous to that of silylidene ($\text{H}_2\text{C}=\text{Si}$) and germylidene ($\text{H}_2\text{C}=\text{Ge}$), although the level of detail obtainable from the present spectra is compromised by the complicating presence of 10 tin isotopes in natural abundance and the limited extent of the $\tilde{B} - \tilde{X}$ spectra of $\text{H}_2\text{C}=\text{Sn}$ and $\text{D}_2\text{C}=\text{Sn}$.

This is the author's peer reviewed, accepted manuscript. However, the online version of record will be different from this version once it has been copyedited and typeset.
PLEASE CITE THIS ARTICLE AS DOI:10.1063/5.0127449

ACKNOWLEDGEMENTS

The authors thank Gretchen Rothschof for her contributions to the early experimental work. M. G. acknowledges the support of a Jordanian Fulbright Scholar Research Award. This research was funded by Ideal Vacuum Products.

AUTHOR DECLARATIONS

Conflict of interest

The authors have no conflicts to disclose.

DATA AVAILABILITY

The data that support the findings of this study are available within the article.

This is the author's peer reviewed, accepted manuscript. However, the online version of record will be different from this version once it has been copyedited and typeset.
PLEASE CITE THIS ARTICLE AS DOI:10.1063/5.0127449

References

1. J. A. DeVine, M. L. Weichman, B. Laws, *et al.* *Science* **358**, 336 (2017).
2. W. W. Harper, E. A. Ferrall, R. K. Hilliard, S. M. Stogner, R. S. Grev and D. J. Clouthier, *J. Am. Chem. Soc.* **119**, 8362 (1997).
3. H. Leclercq and I. Dubois, *J. Mol. Spectrosc.* **76**, 39 (1979).
4. W. W. Harper, K. Waddell and D. J. Clouthier, *J. Chem. Phys.*, **107**, 8829 (1997).
5. D. A. Hostutler, T. C. Smith, H. Li and D. J. Clouthier, *J. Chem. Phys.*, **111**, 950 (1999).
6. T. C. Smith, H. Li and D. J. Clouthier, *J. Chem. Phys.*, **114**, 9012 (2001).
7. D. A. Hostutler, D. J. Clouthier, and S. W. Pauls, *J. Chem. Phys.*, **116**, 1417 (2002).
8. T. C. Smith, C. J. Evans and D. J. Clouthier, *J. Chem. Phys.*, **118**, 1642 (2003).
9. S.-G. He, B. S. Tackett and D. J. Clouthier, *J. Chem. Phys.*, **121**, 257 (2004).
10. R. K. Hilliard and R. S. Grev, *J. Chem. Phys.* **107**, 8823 (1997).
11. H. Harjanto, W.W. Harper, and D. J. Clouthier, *J. Chem. Phys.* **105**, 10189 (1996).
12. W. W. Harper and D. J. Clouthier, *J. Chem. Phys.* **106**, 9461 (1997).
13. D. L. Michalopoulos, M. E. Geusic, P. R. R. Langridge-Smith, and R. E. Smalley, *J. Chem. Phys.* **80**, 3556 (1984).
14. R. D. Anderson and D. H. Taylor, *J. Phys. Chem.* **56**, 161 (1952).
15. R. Tarroni and D. J. Clouthier, *J. Chem. Phys.* **153**, 014301 (2020).
16. M. J. Frisch, G. W. Trucks, H. B. Schlegel *et al.*, Gaussian 09, Revision A.02, Gaussian, Inc., Wallingford, CT, 2004.
17. A. D. Becke, *J. Chem. Phys.* **98**, 5648 (1993).

This is the author's peer reviewed, accepted manuscript. However, the online version of record will be different from this version once it has been copyedited and typeset.
PLEASE CITE THIS ARTICLE AS DOI:10.1063/5.0127449

18. C. Lee, W. Yang, and R. G. Parr, *Phy. Rev. B* **37**, 785 (1988).
19. T. H. Dunning, Jr., *J. Chem. Phys.* **90**, 1007 (1989).
20. K. A. Peterson, *J. Chem. Phys.* **119**, 11099 (2003).
21. A. Bundhun, M. R. Momeni, F. A. Shakib, P. Ramasami, P. P. Gaspar and H. F. Schaefer III, *RSC Adv.* **6**, 53749 (2016).
22. P-C. Wu and M-D. Su, *Inorg. Chem.* **50**, 6814 (2011)
23. T. C. Smith and D. J. Clouthier, *J. Chem. Phys.* **148**, 024302 (2018).
24. D. S. Yang, M. Z. Zgierski, A. Bérces, P. A. Hackett, P. N. Roy, A. Martinez, T. Carrington, Jr., D. R. Salahub, R. Fournier, T. Pang, and C. Chen, *J. Chem. Phys.* **105**, 10663 (1996).
25. E. V. Doktorov, I. A. Malkin, and V. I. Man'ko, *J. Mol. Spectrosc.* **64**, 302 (1977).
26. J. J. Smith and B. Meyer, *J. Mol. Spectrosc.* **27**, 304 (1968).
27. A. Fatah, R. El Ayoubi, H. Gornitzka, H. Ranaivonjatovo and J. Escudié, *Eur. J. Inorg. Chem.*, 2007 (2008).
28. K. M. MacKay in *The Chemistry of Organic Germanium, Tin and Lead Compounds* (Ed.: S. Patai), Wiley, Chichester, vol. 1, ch. 2, (1995).
29. P. R. Bunker and P. Jensen, *J. Chem. Phys.* **79**, 1224 (1983).
30. D. J. Clouthier and D. A. Ramsay, *Annu. Rev. Phys. Chem.* **34**, 31 (1983).
31. R. D. Brown, P. D. Godfrey, D. McNaughton and P. R. Taylor, *J. Mol. Spectrosc.* **120**, 292 (1986).
32. H. Beckers, Y. S. Kim and H. I. Willner, *Inorg. Chem.* **47**, 1693 (2008)
33. S. M. Stogner and R. S. Grev *J. Chem. Phys.*, **108**, 5458 (1998).
34. J. A. Frey, R. Leist, C. Tanner, H.-M. Frey, and S. Leutwylera, *J. Chem. Phys.*, **125**,

This is the author's peer reviewed, accepted manuscript. However, the online version of record will be different from this version once it has been copyedited and typeset.
PLEASE CITE THIS ARTICLE AS DOI:10.1063/5.0127449

114308 (2006).

